LAWRENCE
LIVERMORE
NATIONAL
LABORATORY

UCRL-JC-144727-REV-1

Nuclear Fusion in Gases of Deuterium Clusters and Hot Electron Generation in Droplet Sprays Under Irradiation With An Intense Femtosecond Laser

T. Ditmire, J. Zweiback, T. E. Cowan, G. Hays, K. B. Wharton, J. K. Crane, S. C. Wilks, R. A. Smith, T. D. Donnelly, M. Rust, I. Weiner, M. Allen

July 18, 2001

Super-Intense Laser Atom Physics, Han-Sur, Lesse, Belgium, September 24-30, 2000

This work was performed under the auspices of the U.S. Department of Energy by University of California, Lawrence Livermore National Laboratory under Contract W-7405-Eng-48.

NUCLEAR FUSION IN GASES OF DEUTERIUM CLUSTERS AND HOT ELECTRON GENERATION IN DROPLET SPRAYS UNDER IRRADIATION WITH AN INTENSE FEMTOSECOND LASER

T. Ditmire, J. Zweiback, T. E. Cowan, G. Hays, K. B. Wharton, J. K Crane, S. C. Wilks
Laser Program
Lawrence Livermore National Laboratory
Livermore, CA 94550 USA

R. A. Smith
Imperial College of Science Technology and Medicine,
Blackett Laboratory, London, SW7 UK

T. D. Donnelly, M. Rust, I. Weiner
Department of Physics
Harvey Mudd College
Claremont, CA USA

M. Allen
Department of Nuclear Engineering
University of California
Berkeley, CA USA

1. Nuclear Fusion from Exploding Deuterium Clusters

1.1 INTRODUCTION

A number of experiments have been conducted in recent years examining the interactions of intense femtosecond laser pulses with large van der Waals bonded clusters. Most experiments indicate that these interactions can be very energetic, with a variety of experimental manifestations. Studies from a few years ago revealed that very bright x-ray emission in the 100 to 5000 eV range resulted from the plasmas produced from the interaction of pulses focused to intensity between 10^{16} and 10^{18} W/cm^2 into gas jets that contained rare gas atomic clusters of a few hundred to a few thousand atoms each [1, 2]. This bright x-ray production resulted from the efficient coupling of intense laser light into the cluster gas, strong coupling that was found to be absent when irradiating monatomic gas of similar average density at these intensities. This efficient coupling

was confirmed by subsequent measurements of laser energy absorption in clustering gases [3, 4]. In fact, these experiments illustrated that nearly 100% of an intense laser pulse could be absorbed by a modest average density gas jet (~10^{19} cm^{-3}) within a few mm of propagation length when clusters were present in the gas. This greatly enhanced absorption arises from the fact that the density within the clusters is high, nearly that of a solid, and can therefore exhibit the large absorption efficiency usually associated with solid targets [5].

The laser absorption measurements indicated that many keV of energy per atom were being deposited in the clustering gas. The mechanisms and dynamics of this energy deposition by femtosecond pulses in individual clusters has also been examined by a number of groups. These studies have included measurement of ionization charge states produced in the cluster [6-8], pump-probe and pulsewidth experiments which have shown that the clusters disassemble on a picosecond time scale [9], and photo electron energy measurements which indicated that multi-keV electrons were ejected from large (>1000 atom) Xe clusters [10]. Perhaps most remarkable, has been the discovery that these large clusters, when irradiated at intensity above 10^{15} W/cm^2, also eject ions with substantial kinetic energy. In fact, ions with energy as high as 1 MeV have been seen from exploding Xe clusters [8].

This large release of kinetic energy in fast ions can be harnessed to drive nuclear fusion between deuterium ions if deuterium clusters are irradiated in a gas of sufficient average density to permit collision between ions ejected from different clusters in the gas. Indeed, we recently observed these fusion reactions in gases containing deuterium clusters of roughly 5 nm diameter [11]. In this section we report on a detailed series of measurements of fusion yield from these deuterium cluster explosions and show that, while total fusion yield is modest, the fusion efficiency can be substantial, over 10^5 fusion neutrons per joule of laser energy.

In our experiment a high intensity, ultrafast laser pulse is focused into a gas jet of deuterium clusters, rapidly heating the inertially confined clusters before they can expand. These clusters subsequently explode, ejecting energetic ions. This process creates a plasma filament with a diameter roughly that of the laser focus (~100 μm) and a length comparable to the extent of the gas jet plume (~ 2 mm). The fast deuterium ions ejected from the exploding clusters can then collide with ions ejected from other clusters in the plasma. If the ion energy is high enough (greater than a few tens of keV), D+D nuclear fusion events can occur with high probability. The well known signature of this process arises from one branch of the fusion reaction, $D + D \rightarrow He^3 + n$, in which a neutron is released with 2.45 MeV of energy.

The previous experiments on cluster explosions [8] indicated that large deuterium clusters ionized at high intensity should produce the high ion energies required for fusion. Though large, high Z clusters typically exhibit a "plasma-like" hydrodynamic explosion due to the fact that space charge forces confine many of the photo ionized electrons to the body of the cluster [5], low-Z, medium size (~1000 atoms per cluster) D_2 clusters can be stripped of all of their electrons during the laser pulse, before the cluster explodes. In this case, essentially a pulse Coulomb explosion of the deuterium cluster result. With deuterium cluster sizes of greater then a few tens of angstroms, fully

stripping the cluster with the laser field will result in the explosion of ions with energies greater than a few keV.

1.2 EXPERIMENTAL APPARATUS

Our experiment uses a 10 Hz, Ti:sapphire, chirped pulse amplification laser delivering 120 mJ of laser energy per pulse with 35 fs pulse width and wavelength of 820 nm. This laser was focused into the exit of a deuterium gas jet with an f/12 lens. Because the van der Waals forces between deuterium molecules are weak, the gas jet was cryogenically cooled by flowing cooled nitrogen through a jacket surrounding the gas jet body to -170° C [12], producing large clusters in the D_2 gas. The laser spot size within the gas jet varied from roughly 20 to 130 μm depending on the focal spot position, with respect to the gas jet nozzle. Consequently the peak laser intensity was between 5 x 10^{17} W/cm^2 and 2 x 10^{16} W/cm^2 for all of the experiments described here.

To estimate the deuterium cluster size in our gas jet, we conducted Rayleigh scattering measurements in the jet by passing low energy (< 0.1 mJ) 532 nm pulses from a frequency doubled, Q-switched Nd:YAG laser (pulse width 10 ns) through the plume of the gas jet. The Rayleigh scattered light from cluster formation was imaged 90 degrees from the laser propagation axis. From the observed onset of Rayleigh scattering, we can determine the onset of large cluster formation in the jet. In addition, using independent measurements of the average gas density (see below), estimates for the throughput and detection sensitivity, and the Rayleigh scatter cross section, we are able to estimate the average cluster size in the jet. Measured scattering as a function of gas jet pressure is illustrated in Figure 1 when the gas jet backing temperature is 100K. From these data it can be seen that the scattering signal is a strong function of the jet pressure and that no significant cluster formation is observed until the jet pressure increases above 20 atm. A strong variation with gas jet backing pressure is also observed.

1.3 FUSION EXPERIMENTAL RESULTS

To determine the efficiency with which the 120 mJ, femtosecond laser pulse was coupled into the deuterium clusters we measured the absorption efficiency of the laser pulse within the deuterium cluster gas jet. To do this, we measured the transmitted laser energy collected within an f/3 cone (to collect all potentially refracted light from the f/12 cone) with a large aperture lens and calorimeter. We monitored backscattered light with a photodiode (very little was observed in these experiments). We also estimated scattered light using a CCD camera and collection lens monitoring light scattered 90° from the laser propagation direction perpendicular to the laser polarization direction (the direction of maximum Rayleigh scatter). Extrapolating into 4π we determined that the scattered light was negligible (< 1 mJ),

The absorption as a function of gas jet reservoir backing pressure is illustrated in Figure 2 when the gas has been initially cooled to -170° C (the case in which we observe large D_2 cluster formation). As can be seen, when the deuterium gas jet pressure rises to

>30 atm, nearly 90% of the laser energy is deposited in the plasma. This is in sharp contrast to the energy deposition efficiency of the laser in pure D_2 molecular gas (the case when the gas jet reservoir is at 20° C), a case also plotted in Figure 2. In this case very little (< 5%) of the laser energy is deposited in the plasma, illustrating the importance of the laser/cluster interaction in heating the D_2 plasma.

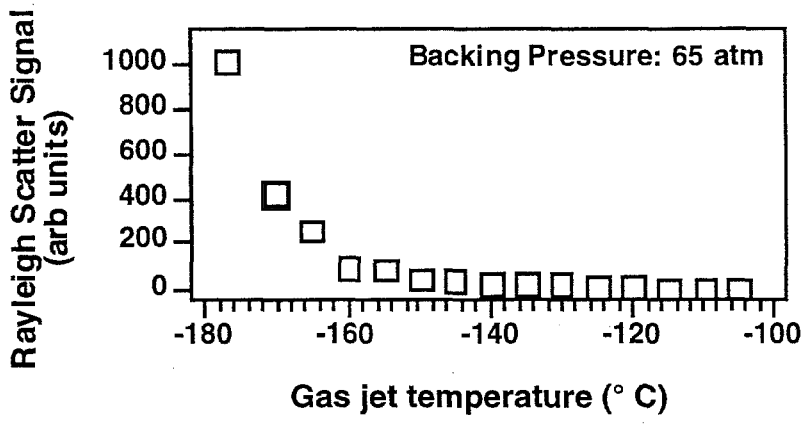

Figure 1: Measured Rayleigh scatter signal in the deuterium gas jet as a function of gas jet backing pressure. The reservoir temperature was 100K.

To detect the production of DD fusion neutrons in these experiments we employed various arrays of neutron sensitive scintillator detectors at various distances from the interaction point. Though different detector configurations were employed, the majority of the data presented below were collected with detectors consisting of 10 x 10 cm^2 scintillator slabs of 7mm thickness coupled to PMTs via light pipes. These detectors were located outside the vacuum interaction chamber and were shielded with 6 mm of lead. The time of flight of particles from the time the laser irradiates the plasma is recorded. Each neutron detector was operated in a mode such that a particle was detected every few laser shots, permitting a determination of the flight time of each detected particle with < 1 ns accuracy.

With these neutron detectors we detected the presence of substantial numbers of MeV energy particles when the gas was backed with cooled deuterium at a pressure of 65 atm and a reservoir temperature of -170 C. A characteristic time-of-flight spectrum of particles detected on a neutron detector located 54 cm from the source is illustrated in Figure 3. These time-of-flight spectra were acquired by accumulation of particle hits over ~ 10,000 laser shots. In these data, a distinct peak occurs in the detected TOF spectrum at the position expected for 2.45 MeV neutrons (which have a flight time of 46 ns/m) at 24.5 ns for 54 cm separation. This measurement confirms the presence of DD fusion reactions in the cluster plasma. We also confirmed that all detected particles on the neutron detectors disappear when hydrogen clusters were made in the jet in lieu of the

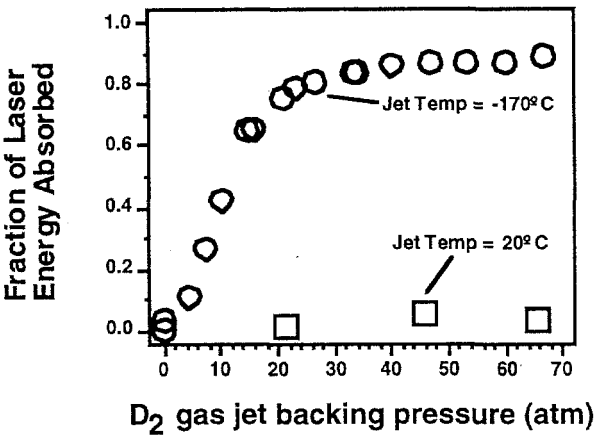

Figure 2: Measured absorption of the 35 fs pulse in the deuterium gas jet as a function of backing pressure for two different jet temperatures.

deuterium clusters (a measurement taken over 50 laser shots assuring better than 1 part in 10^8 that no neutrons were produced when hydrogen replaces deuterium). Furthermore, we found that the fusion neutron production disappeared when deuterium clusters where absent in the D_2 gas jet (when the jet was not cooled). We observed no neutron production in the gas jet with temperatures higher than -120° C, the temperature at which we no longer observe large cluster formation via Rayleigh scattering.

The signal seen in these spectra after the main neutron peak arise from neutron scattering from the gas jet and vacuum chamber walls. We have conducted estimates of the expected scattered neutron signal and have confirmed that these longer time detected particles are consistent with scattered neutrons from material surrounding the fusion plasma, such as the gas jet body and vacuum chamber walls. We also see an occasional hit early in time. It is likely that these are hard x-rays produced from fast electrons released in the laser/cluster interactions. These fast electrons can produce bremsstrahlung photons in the surrounding material, including the stainless-steel gas jet body.
However, these gammas are rare and the vast majority of the signal observed in this experiment are from the fusion neutrons.

Also shown in figure 3 is the neutron TOF distribution very close to the source. This distribution was collected using a very thin (1.5 mm) scintillator directly coupled to the PMT detector. This detector was optimized to yield very high time resolution, which was measured with an x-ray flash to be <250 ps. From this we can derive information on the duration of the neutron pulse width. As can be seen in figure 3, the pulse duration measured with this device at a distance of 9 cm is well under 1 ns. Detailed deconvolution of the neutron pulse with the intrinsic time response of the detector indicated that the neutrons had duration 650 ps here. The 55 cm data indicate that the neutrons have a duration of 1.4 ns. This broadening with distance is a result of Doppler-like broadening of the neutron energy around 2.45 MeV resulting from the ion temperature. These measurements also indicate that the fusion burn time at the plasma is likely < 500 ps.

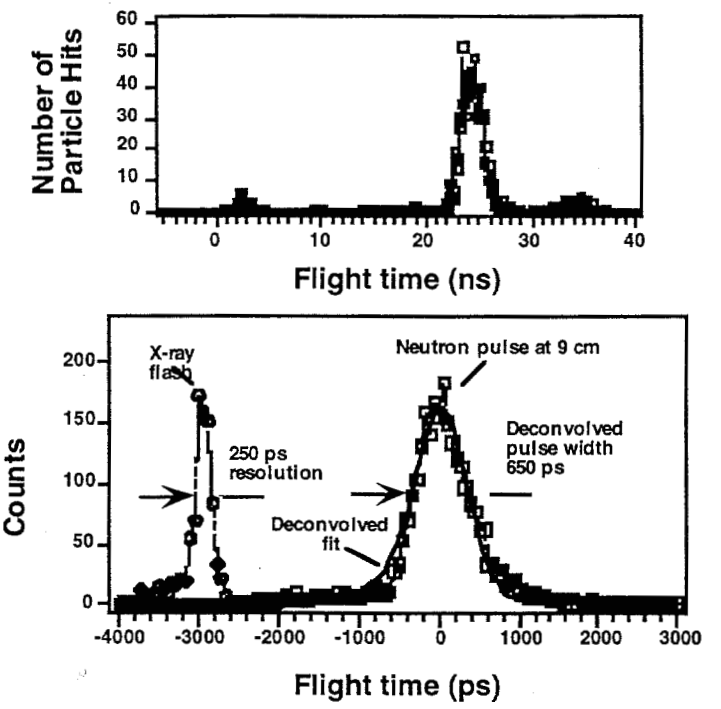

Figure 3: Time-of-flight spectrum of particles detected on an n detector located 54 cm from the source (top) and TOF spectrum 9cm from source (bottom).

To measure the change in neutron yield as different parameters were varied, an additional plastic scintillator detector was placed near the plasma in an re-entrant flange to subtend a large solid angle. It subtended an angle of 0.3 ster and was placed 20 cm from the deuterium plasma. Because the time-of-flight data indicate that there is no noticeable x-ray flash and that virtually all of the detected particles are neutrons, we obtained a shot by shot measure of the fusion yield from the PMT signal. The detection efficiency was calibrated against the other TOF detectors operating in single particle detection mode. We also calibrated the yield by measuring the average pulse height produced when single neutrons struck the detector. Both methods yielded nearly equal values for the yield calibration.

Using this detector, we measured the yield as a function of various parameters. Most importantly, we wish to optimize the fusion yield. Because the fusion cross section is very strongly dependant on the ion energy, small increases in ion kinetic energy from the exploding clusters should yield dramatic increases in the fusion yield. In a Coulomb explosion picture of the fast ion generation, the average ion energy from an exploding sphere of ions that have had their electrons stripped is given by $Qn_c e^2 a^2/5\varepsilon_0$ where Q is the total charge on the cluster, n_c is the initial cluster ion density and a is the cluster radius. Thus, we expect that increasing the cluster size in the jet will (to a certain point) increase the ion energy and hence the fusion yield.

To examine this, we used the well known fact that cluster size from a gas jet expansion is a strong function of the initial reservoir temperature [13]. We varied the

temperature of our jet by using liquid nitrogen to cool the jet over a range roughly >100 K and then used liquid helium to further cool the jet. We measured the temperature of the jet body with a thermocouple. Though it did not directly register the temperature of the gas, it acted as good parameter to characterize the gas cooling.

The measured average size of clusters from the jet as a function of measured temperature is shown in figure 4a. We can produce average cluster sizes up to 10 nm (though it is likely that there is a broad distribution of clusters in the jet.) The measured fusion yield as a function of measured temperature is shown in figure 4b. We observe

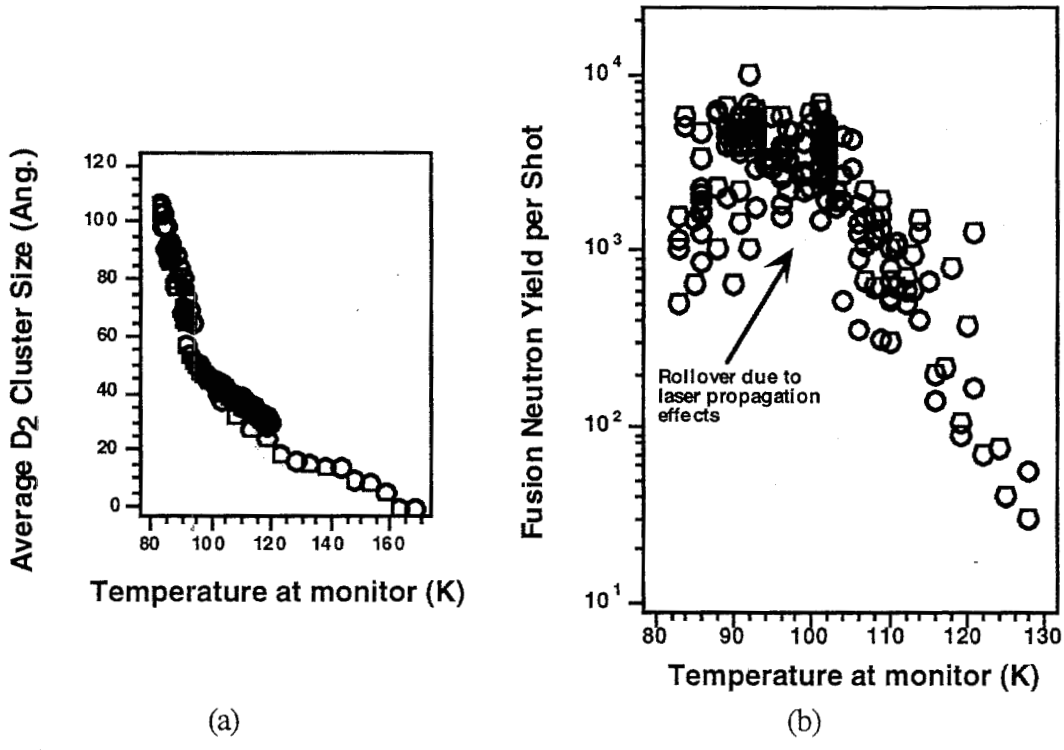

Figure 4: (a) Measured average size of clusters from the jet as a function of measured temperature (b) Measured fusion yield as a function of measured temperature

the expected rapid increase in fusion yield as the cluster size increases with lower temperature down to a temperature of roughly 100K. Detailed analysis of these data indicate that the observed rise in yield is, indeed, consistent with a Coulomb explosion model. The roll over in fusion yield at temperatures below 100 K results from laser propagation effects in the gas jet. Other measurements in this parameter regime indicate that this roll over results from the fact that the laser is strongly absorbed in thedistribution of gas out in front of the center of the plume [14]. As the cluster size is increased, this gas more effectively depletes the laser pulse as it propagates toward the center of the plume preventing further rise in yield.

2. Hot Electron Generation from intense Irradiation of Wavelength Scale Particles

2.1 INTRODUCTION

The interesting phenomena seen in the explosions of nm scale clusters suggest that there might be interesting effects in the intense irradiation of somewhat larger particles. One area of potential interest is in examining hot electron generation from intense irraction of ultrafast laser pulses with particles whose size approaches that of the laser's wavelength. Over the last few years, experimental studies have shown that sub-picosecond to femtosecond lasers focused to intensities of 10^{17} to 10^{20} W/cm^2 on solid targets will, indeed, accelerate substantial numbers of electrons to high energy, and that these fast electrons can produce large fluxes of hard x-rays via bremsstrahlung emission in the target [15]. A number of such experiments have observed photons emitted in the > 1 MeV energy range indicating that such focused laser intensity can accelerate electrons to relativistic temperatures of several hundred keV to well over an MeV [16].

The mechanisms leading to the acceleration of fast electrons responsible for the hard x-rays in laser-solid interactions has been the topic of many experimental and theoretic studies over the past two decades. At intensities approaching 10^{18} W/cm^2 the ponderomotive potential of light with wavelength around 1 μm nears 100 keV and direct acceleration of electrons can occur through electron interactions with the laser field at a plasma surface (Brunel heating [17]) or through **J x B** heating [18]. In addition, when a long scale-length (many wavelength) preformed plasma exists in front of the target, collective electron oscillations driven by resonance absorption or stimulated Raman scattering can also play an important role in accelerating the electrons. Generally, both theoretical and experimental evidence indicates a linear or sub-linear scaling of fast electron temperature with laser ponderomotive potential [19] with calculated hot electron distributions for p-polarized pulses incident on solids exhibiting temperature four to five times the laser ponderomotive potential.

The extension of these studies to small particles is motivated by the fact that linear absorption and scattering of light by particles whose size is comparable to the light wavelength (around 1 μm) can be increased over that of bulk media from enhancements in the light field surrounding the sphere, so called Mie resonances. Thus we might expect that the dynamics of laser driven electron motion will be quite different around such a wavelength scale sphere, and that vacuum heating of hot electrons will take on a different character. To study this effect we measured hard x-ray spectra from a target consisting of micron scale droplets.

2.2 EXPERIMENTAL RESULTS USING A DROPLET SPRAY

This experiment was performed with the same laser system used in the fusion experiments. For the droplet experiments, 0.12 J of laser energy was focused in vacuum with an f/15 lens to a focal spot of roughly 20 μm diameter ($1/e^2$). Far field

measurements indicate a peak intensity of 7 x 10^{17} W/cm^2. The pre-pulse intensity contrast was ~ 10^{-6} on the 1 ns time scale before the main pulse and was ~ 10^{-4} on the 10 ps time scale. We estimate that plasma pre-expansion from pre-pulse light was well under 1 μm. These pulses were focused onto either a plane, plastic target in P-polarization at an incidence angle of 10° or into a spray of water droplets. Plastic was chosen as the target material because it exhibits a similar density and has a similar Z to water, the target material in our droplet spray.

The water droplet target was produced by an apparatus capable of creating a high density, polydisperse spray containing micron-scale liquid water droplets in vacuum (similar to the apparatus described in ref. [20]). The droplet source consisted of a gas line backed with high pressure argon (at 67 bar), an inert propellant gas, over a liquid reservoir. The line terminated in a solenoid driven pulsed valve with a 750 μm orifice. The valve was pulsed for 500 μs, causing propellant gas carrying liquid droplets to stream through the orifice.

The composition of the spray produced by the device was characterized in vacuum by measuring the angular scattering and attenuation of a continuous wave 543 nm helium-neon laser polarized perpendicular to the scattering plane. The droplet sizes were measured by fitting theoretical Mie scattering curves of the 543 nm light to the data [21]. As the radius of the sphere increases, the ratio of the intensity of light scattered in the forward direction increases relative to that scattered at larger angles, making the angular distribution of scatter a sensitive test of particle size. Relative Mie scattering data were obtained by integrating the observed signal over the entire 500 μs open time. Angular scatter data for the droplet spray used in our experiment is shown in figure 5.

To ascertain the droplet size, we calculate expected scattering angular distributions using a code calculating the differential Mie scattering cross section. We find that we can fit these scattering data if a two size distribution is assumed. A fit with a single size

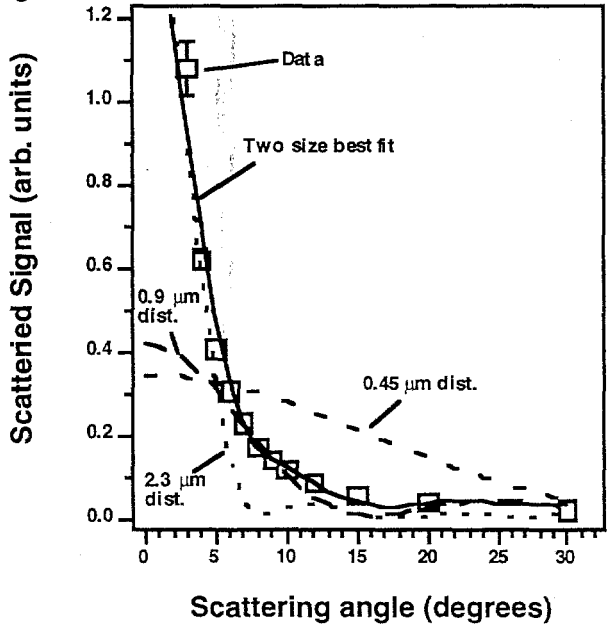

Figure 5: Measured Mie scattering with best fits of droplets in our water spray target

distribution centered at r = 0.9 μm is plotted in the figure. This calculation adequately fits the data at mid-angles (5 – 15 degrees) though it contains oscillations at large angles not seen in the data and does not reproduce the large scattering at small angles. To adequately fit the observed data, we assume a droplet size distribution with a Gaussian profile centered at r = 0.9 μm with a 20% spread (at the 1/e point) with a small additional contribution of droplets with r = 2.3 μm. The large droplets contribute predominately to the small angle scatter signal. The data are reasonably well reproduced by calculation when we assume that 5% of the droplets have an r = 2.3 μm. For comparison, we also show curves for purely r = 2.3 μm droplets as well as small r = 0.45 μm.

The droplet density was determined from light attenuation measurements. With knowledge of the droplet size, and the propagation length of the probe laser through the droplet plume (determined by imaging the scattering onto a CCD), one can use the Mie theory to calculate the average density of particles in the plume. Our measurements indicate that the droplet spray was roughly 2 mm wide and exhibited a density of 6×10^7 droplets/cm^3 (or 7×10^{18} molecules/cm^3). This implies that there are a few tens (10 –100) of droplets in the focal volume per laser shot.

Hard x-rays from the target region, either droplet or planar solid, were observed 90° from the laser propagation axis using detectors employing NaI crystals coupled to photo-multiplier tubes. These detectors were housed in a thick lead casing with an aperture pointed at the target region. X-rays were observed through a 5 mm thick glass window and data were taken with three different filters in front of the detector. We acquired data with an 0.5 cm thick Cu filter and 0.35 cm and 4 cm thick Pb filters. These filters were chosen to yield spectral information in the 100 keV to 1 MeV photon energy range. In addition, data were collected with an unshielded reference detector, filtered by only the 5 mm stainless steel vacuum chamber wall. This detector provided information on x-rays produced with energy above 50 keV and was used to discriminate high and low intensity shots.

Abundant hard x-ray emission was observed from both the solid plastic targets and the water droplet target. The x-ray yield measured from both targets is plotted in figure 6. Here the total x-ray energy deposited in the detector per shot is plotted versus the cut-off energy ($1/e^2$) of each filter. Consequently the data points roughly represent the integrated x-ray yield above this photon energy point. From this illustration it is evident that the total x-ray yield observed from the two kinds of targets is comparable over the 0.1 to 1 MeV energy range. Hard x-rays from the solid target occur due to bremsstrahlung of fast electrons in the bulk material, We further surmise that hard x-ray emission occurs in the droplet target due to bremsstrahlung in the stainless steel droplet jet body from hot electrons produced in the droplets themselves.

While a direct comparison of x-ray yields between these two targets does not yield quantitative information because of the differing mechanisms for producing the bremsstrahlung (plastic as opposed to stainless steel converter for the droplets), it is clear from this figure that the comparable x-ray yields indicate at least roughly comparable hot electron production in the two cases.

To determine the approximate hot electron temperature from these data, we performed simulations of bremsstrahlung production from various exponential electron distributions using the Monte Carlo code, ITS [22]. We calculate hard x-ray spectra from single temperature electron distributions in plastic and in solid iron (to model the droplet x-ray production) and account for the target geometry and direction of detection (90° to the laser). We assume a single temperature Maxwellian electron energy distribution and numerically generated a photon spectrum, $f(E_\gamma)dE_\gamma$ where E_γ is the photon energy. These results were then fit to the data points using a least squares analysis by varying the initial hot electron temperature using the fact that the signal measured in each filtered detector is proportional to $\int E_\gamma\, T(E_\gamma) f(E_\gamma)\, dE_\gamma$ where $T(E_\gamma)$ is the transmission of each filter as a function of x-ray wavelength.

The best spectrum for each of the targets is shown also in figure 6. We find that the best fit hot electron temperature of the solid plastic target is 400 keV with a single standard deviation of ±100 keV. The droplet target data exhibited a best fit with a 700 keV hot electron temperature and a standard deviation of ±150 keV. The temperature of the solid target is consistent with previously published hot electron temperature measurements in this intensity range (approaching 10^{18} W/cm^2) [16] however, the hot electron temperature inferred from the droplet measurements is nearly twice that inferred from the solid target.

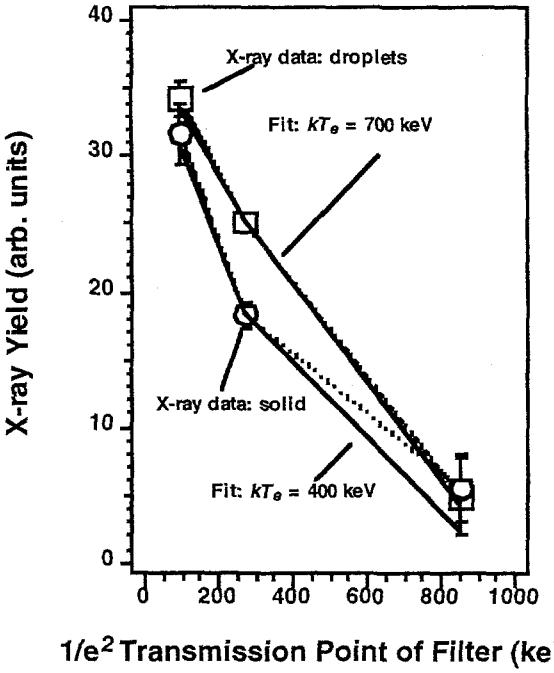

Figure 6: Measured hard x-ray yield from the droplet and solid targets with best fit electron temperatures.

2.3 SIMULATION RESULTS

To understand these observed differences, we have conducted 2D particle-in-cell simulations of a 30 fs pulse irradiating a round solid density plasma and planar solid targets at a peak intensity of 5 x 10^{17} W/cm^2. These simulations were conducted with

the code ZOHAR [23] in which solid material was approximated as an overdense, 5 x 10^{22} cm^{-3} plasma. In the planar target calculations, the laser field was p-polarized and was incident at an angle of 19°. An example of the field distribution calculated around a one micron spherical (droplet) plasma is shown as a contour plot in figure 7 near the peak of the laser pulse envelope. As exhibited in figure 7, we observe the presence of enhanced regions of electric field near the droplet surface in a roughly dipole pattern (i.e. both at the surface of incidence as well as the back surface). This arises from the oscillating electrons perpendicular to the laser **k** vector.

The hot electron spectra produced from simulations of the droplet and the planar slab are shown in figure 8. The calculation predicts a hot electron temperature of 125 keV from the flat target and a temperature of 240 keV from the droplet, nearly a factor of two higher than the planar slab, much like the enhancement observed in the experiments. Though these electron temperatures are somewhat lower than observed in the experiment, they do confirm that the electron temperature resulting from the interaction with a small sphere is significantly higher than in the interaction with a planar slab.

In the simulation, the majority of the hot electron production is due to Brunel-type heating of the oscillating electrons at the surface in both the droplet and the slab target simulations. However, the enhanced electron heating observed in the case of the particle appears to arise from the differing electron trajectories possible around the droplet target geometry. In the case of the slab target, electrons acquire energy from the laser field through acceleration in vacuum toward the slab surface. Thus, most electrons acquire substantial velocity in the direction perpendicular to the slab surface (the direction in which the field adiabaticity is broken). In the droplet simulation, however, the laser field diffracts around the droplet and electrons can undergo numerous surface penetrations at various angles through the surface of the plasma sphere. In this case, the particle plasma is large enough to shield the laser field (unlike the case of the much smaller nm scale clusters studied) and the electrons can acquire substantial momentum, both parallel and perpendicular to the laser **k** direction.

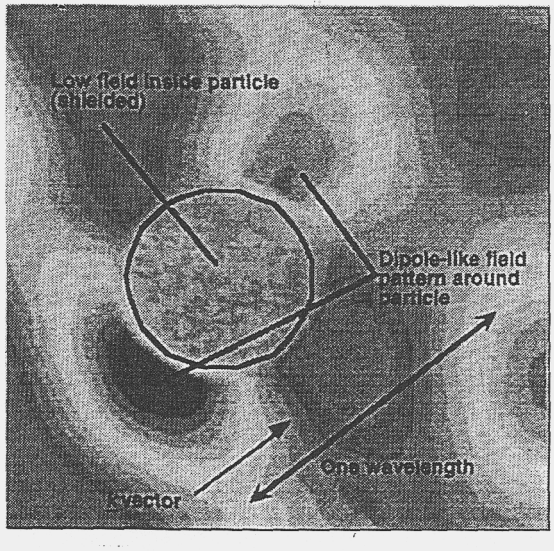

Figure 7: Field distribution calculated around a one micron spherical plasma.

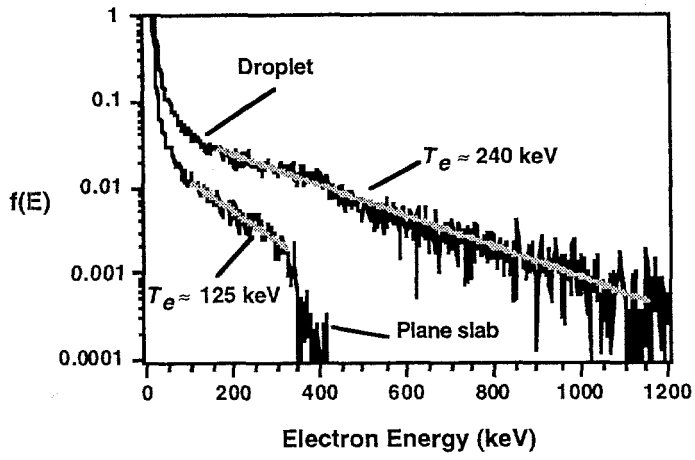

Figure 8: Hot electron spectra produced from simulations of the droplet and the planar slab with best fit temperatures.

3. Conclusion

In conclusion, we have observed the production of 2.45 MeV deuterium fusion neutrons when a gas of deuterium clusters is irradiated with a 120 mJ, 35 fs laser pulse. When the focal position is optimized, we have observed as many as 10^4 neutrons per laser shot. This yield is consistent with some simple estimates for the fusion yield. We also find that the fusion yield is a sensitive function of the deuterium cluster size in the target jet, a consequence of the Coulomb explosion origin of the fast deuterons. We also find that the neutron pulse duration is fast, with a characteristic burn time of well under 1 ns. This experiment may represent a means for producing a compact, table-top source of short pulse fusion neutrons for applications.

Furthermore, we have measured hard x-ray yield from femtosecond laser interactions with both solid and micron scale droplet targets. Strong hard x-ray production is observed from both targets. However, the inferred electron temperature is somewhat higher in the case of irradiation of the droplets. These data are consistent with PIC simulations. This finding indicates that quite unique hot electron dynamics occur during the irradiation of wavelength scale particles by an intense laser field and likely warrants further study

We would like to acknowledge many useful conversations with John Perkins and Howard Powell as well as the technical assistance of Vince Tsai, Gerry Anderson and Rich Shuttlesworth. This work was supported by the Department of Energy under contract W-7405-Eng-48.

4. References

1. McPherson, A., Thompson, B. D., Borisov, A. B., Boyer, K., and Rhodes, C. K. (1994) Multiphoton-induced X-Ray Emission at 4-5 keV from Xe Atoms with Multiple Core Vacancies, *Nature* **370**, 631 .
2. Ditmire, T., Donnelly, T. D., Falcone, R. W., and Perry, M. D. (1995) Strong X-ray Emission from High Temperature Plasmas Produced by Intense Irradiation of Clusters, *Phys. Rev. Lettt.* **75**, 3122.
3. Ditmire, T., Smith, R. A., Tisch, J. W. G., and Hutchinson, M. H. R. (1997) Absorption of High Intensity Laser Pulses in Gases of Clusters, *Phys. Rev. Lett.* **78**, 3121 .
4. Kondo, K., Borisov, A. B., Jordan, C., McPherson, A., Schroeder, W. A., Boyer, K., and Rhodes, C. K. (1997) Wavelength Dependence of Multiphoton-induced Xe(M) and Xe(L) Emissions from Xe Clusters, *J. Phys. B: At. Mol. Opt. Phys.* **30**, 2707 .
5. Ditmire, T., Donnelly, T., Rubenchik, A. M., Falcone, R. W., and Perry, M. D. (1996) The Interaction of Intense Laser Pulses with Atomic Clusters, *Phys. Rev. A* **53**, 3379 .
6. Lezius, M., Dobosz, S., Normand, D., and Schmidt, M. (1997) Hot Nanoplasmas from Intense Laser Irradiation of Argon Clusters, *J. Phys. B: At. Mol. Opt. Phys.* **30**, L251 .
7. Snyder, E. M., Wei, S., Purnell, J., Buzza, S. A., and Castleman. Jr., A. W. (1996) Femtosecond Laser-Induced Coulomb Explosion of Ammonia Clusters, *Chem. Phys. Lett.* **248**, 1 .
8. Ditmire, T., Tisch, J. W. G., Springate, E., Mason, M. B., Hay, N., Smith, R. A., Marangos, J., and Hutchinson, M. H. R. (1997) High-Energy Ions Produced in Explosions of Superheated Atomic Clusters, *Nature (London)* **386**, 54 .
9. Zweiback, J., Ditmire, T., and Perry, M. D. (1999) Femtosecond Time Resolved Studies of the Dynamics of Noble Gas Cluster Explosions, *Phys. Rev. A* **59**, R3166 .
10. Shao, Y. L., Ditmire, T., Tisch, J. W. G., Springate, E., Marangos, J. P., and Hutchinson, M. H. R. (1996) Multi-keV Electron Generation in the Interaction of Intense Laser Pulses with Xe Clusters, *Phys. Rev. Lett.* **77**, 3343.
11. Ditmire, T., Zweiback, J., Yanovsky, V. P., Cowan, T. E., Hays, G., and Wharton, K. B. (1999) Nuclear Fusion from Explosions of Femtosecond-Laser Heated Deuterium Cluster, *Nature* **398**, 489.
12. Smith, R. A., Ditmire, T., and Tisch, J. W. G., (1998) Characterization of a Cryogenically Cooled High-Pressure Gas Jet for Laser/Cluster Interaction Experiments, *Rev. Sci. Instrum.* **69**, 3798.
13. Hagena, O.F. and Obert, W. (1972) Cluster Formation in Expanding Supersonic Jets: Effect of Pressure, Temperature, Nozzle Size, and Test Gas, *J. Chem. Phys.* **56**, 1793.
14. Zweiback, J., Smith, R. A., Yanovsky, V. P., Cowan, T. E., Hays, G., Wharton, K. B. and Ditmire, T. (1999) Nuclear Fusion from Coulomb Explosions of D_2 Clusters Ionized by a Femtosecond Laser, in *Multi-photon Processes* eds. R. Freeman, K. Kulander, L. DiMauro.
15. Kmetec, J. D., et al.(1992) *Phys. Rev. Lett.* **68**, 1527.
16. Chichkov, B. N., et al. (1996) *Applied Physics Letters* **68**, 2804-2806 .
17. Brunel, F. (1987) *Phys. Rev. Lett.* **59**, 52.
18. Wilks, S. C., Kruer, W. L., Tabak, M., and Langdon, A. B. (1992) *Phys. Rev. Lett.* **69**, 1383 .
19. Gibbon, P. (1994) *Phys. Rev. Lett.* **73**, 664.
20. Mountford, L. C., Smith, R. A., and Hutchinson, M. H. R. (1998) *Rev. Sci. Intrs.* **69**, 3780.
21. Kerker, M., (1969) Scattering of Light and Other Electromagnetic Radiation. Academic, New York. .
22. Halbleib, J. A., and Mehlhorn, T. A. (1986) *Nucl. Sci. Eng.* **92**, 338.
23. Langdon, A. B. and Lasinski, B. F. (1976) Methods in Computational Physics. Vol. 16, Academic Press, New York p. 327.